Structural study of columnar liquid-crystalline phases in homologous series of tetrapalladium organyls†

Benoît Heinrich,[a,b] Klaus Praefcke*[a] and Daniel Guillon*[b]

[a]*Institute of Organic Chemistry, Technische Universität Berlin, D-10623 Berlin, Germany*

[b]*Institut de Physique et de Chimie des Matériaux de Strasbourg, Groupe des Matériaux Organiques, UMR 46 CNRS-ULP, 23, rue du Loess, BP 20 CR, F-67037 Strasbourg Cedex, France*

The molecular organisation within liquid-crystalline columnar phases shown by a series of tetrapalladium organyls has been investigated by varying systematically the number and length of the alkoxy substituents connected to their flat core. Four different columnar phases were observed and studied by polarising microscopy, DSC, X-ray diffraction and dilatometry. In two types of *C*2*mm* rectangular centred phases and in an oblique *P*2 phase, the cores of the columns, formed by the stacking of the roughly rectangular-shaped flat molecular cores, were found to retain the same orientation between neighbouring columns. A transformation of the *C*2*mm* lattice into the rectangular *P*2*gg* lattice was observed at high temperature for the derivatives with long chains. The succession of columnar phases as well as the evolution of the packing geometry within the organyl series is explained in terms of the relation between the aliphatic chain length and that of the longest side of the flat rectangular columnar cores.

Different columnar symmetries and geometries of mesophases can be observed in lyotropic systems, depending on the hydrophilic–hydrophobic balance.[2] In thermotropic systems of disc-like molecules the columnar mesophase structure is related to the flat molecular core structure, but the balance between such stacked flat cores and the aliphatic periphery still plays a major role.[2–5] Thus the contact region between the core of the columns and the aliphatic periphery is given by the molecular core dimensions; this implies that the columnar packing should change when the number of the aliphatic tails or when the coiling of these chains varies. In addition, other geometric features have a large influence on the arrangement of the columns and on the stacking within them, for instance the shape of the flat molecular cores, the length of the aliphatic tails and the grafting positions. In the following, the evolution of the columnar packing induced by modifications in the aliphatic periphery will be discussed for a roughly rectangular-shaped tetrapalladium organyl based flat core. The tetrapalladium organyl with twelve dodecyl chains in the periphery and the tetraplatinum analogue have already been synthesised and studied with respect to their columnar mesomorphism.[6–8] Injected domains of columnar nematic phases were observed in phase diagrams between linear *n*-alkanes and these tetrapalladium (or platinum) organyl derivatives.[8–10]

Materials

Seven homologues of the previously synthesised tetrapalladium organyl series (**12-234**, **10-234** and **14-234**[6,7,10]) were prepared (see Fig. 1). In addition to the ***n*-234** homologous series, for which each benzylidene unit is substituted by three alkoxy chains in positions 2, 3 and 4, three palladium organyls with the benzylidene units disubstituted in positions 2 and 3 (**12-23** and **18-23**) or 2 and 4 (**12–24**) were also prepared. No pure palladium organyl with disubstitution in positions 3 and 4 could be obtained, while monosubstitution in either position led to insoluble products decomposing without melting above 300 °C. The transition temperatures are listed in Table 1. All metal organyls exhibit liquid-crystalline phases with temperature ranges between 150 and 260 °C. The disubstituted organyls have a tendency to show higher melting points and lower clearing points than the trisubstituted ones with the same chain length. In the case of trisubstituted organyls, the broadest liquid-crystalline range and the minimum melting point is found for the metal organyl **10-234**. The width of the liquid-crystalline domain is reduced with increasing chain length.

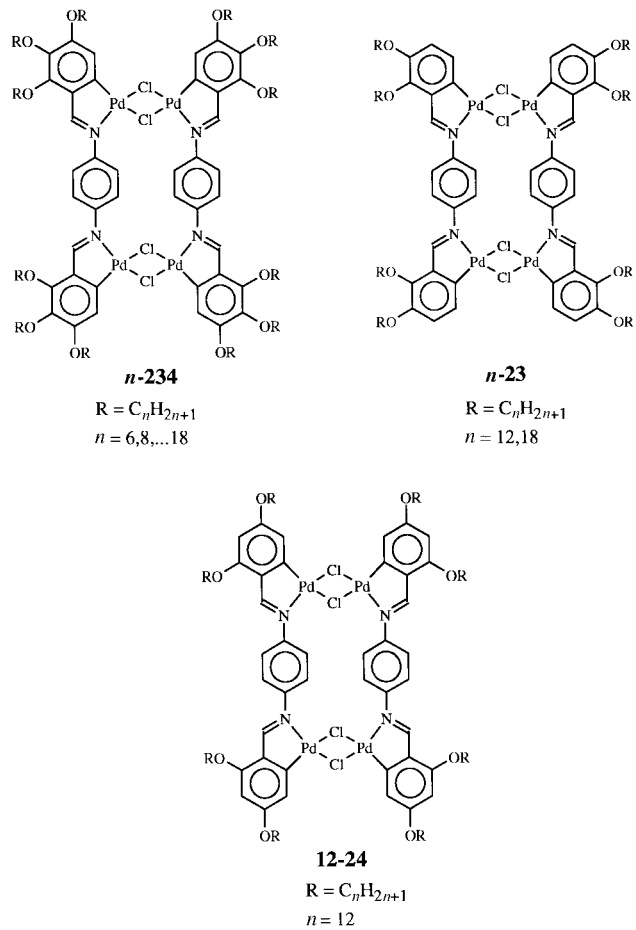

Fig. 1 Formulae of the 10 palladium organyls described in the text

† Part 103 of a series on liquid-crystalline compounds of the group of Berlin. Part 102: ref. 1.

Table 1 Liquid-crystalline polymorphism of the ten palladium organyls described in the text (temperatures are in °C)

mesogen	K		Col1		Col2		Col3		Col4		I
6–234	•	101	•	329	—		—		—		•
8–234	•	76	•	320	—		—		—		•
10–234	•	55	—		•	220[a]	•	316	—		•
12–234	•	70	—		—		•	298	—		•
14–234	•	74	—		—		•	[b]	•	277	•
16–234	•	81	—		—		•	[b]	•	265	•
18–234	•	95	—		—		•	[b]	•	249	•
12–23	•	106	—		—		•	[b]	•	295	•
18–23	•	94	—		—		•	[b]	•	254	•
12–24	•	93	•	257	—		—		—		•

[a]Approximate transition temperature determined from X-ray patterns; transition not visible by DSC. [b]The occurrence of this transition (not visible by DSC) depends on the thermal history of the sample; both phases (Col3 and Col4) may coexist over an extended temperature range.

This is due to the increase of the melting points and to the decrease of the clearing points; both changes are of similar order of magnitude.

No characteristic optical texture could be obtained with polarizing microscopy, either by cooling from the isotropic phase, or by evaporation from a solvent in the mesophase. However, the X-ray diffraction patterns revealed that the liquid-crystalline domain is composed by up to four different columnar phases, labelled Col1–Col4.[8] The Col1 phase occurred for the compounds with the shortest chains, the Col2 phase was observed only for the metal organyl **10-234**. For this homologue a phase transition to the Col3 phase was deduced from the X-ray patterns, although no signal was detected by DSC. Further increasing the chain length resulted in the extension of the Col3 phase domain. The decomposition of the compounds occurred above 250 °C. Nevertheless, for the compounds with the longest chains, a slow and irreversible transformation into the Col4 phase was observed at high temperature. Within the Col1 domain the samples exhibited a tough pasty consistency. Within the Col2 to Col4 domains the viscosity could be compared to that of a viscous oil.

Results and Discussion

Packing of the columns

The packing within the liquid-crystalline phases Col2, Col3 and Col4 consists of a long-range ordered two-dimensional arrangement of columns formed by the neatly piled flat cores, but without any long-range correlation between the positions of the flat cores within the columns. In the following we will call these phases 'disordered' columnar phases. In contrast, the phase Col1 for which long-range correlations between the positions of the flat cores do exist will be called the 'ordered' columnar phase.

Disordered columnar phases (a) *The phases Col2 and Col3.* The phase Col3 was previously investigated for the organyl **12-234**[7] and for a similar organyl, differing only on the nature of the metal (Pt instead of Pd).[8] It was shown that both metal organyls presented the same type of arrangement with almost no differences in the lattice parameters.[8] Indeed, the columnar cores (the cross-section of which is similar to a rectangle of dimensions 12×18 Å) organise themselves in rows with a constant orientation within and between the rows (see Fig. 2). In the previous work,[7] the indexation was performed by considering that the oblique lattices **1**[7] and **2**[8] and the orientation of the cores were determined from the temperature dependence of the lattice parameters.[8] The lattice **3** (containing two columns instead of one) will therefore be considered, since

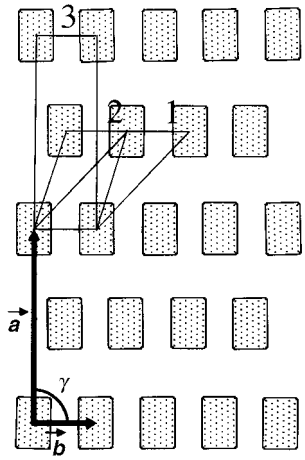

Fig. 2 Structure of the Col3 phase for the palladium organyl **12-234**. It was previously considered as oblique and the indexation was performed with the lattice **1**.[4] A similar platinum organyl, presenting the same structure and very similar lattice parameters, was also considered as oblique and the indexation was performed with the lattice **2**.[6] A re-examination of these results revealed the higher rectangular centred *C*2*mm* symmetry and the indexation presented in the following corresponds to the lattice **3**.

a re-examination of the lattice parameters previously found[7] revealed that the results are compatible with a more complete description of the packing involving a centred rectangular symmetry ($\gamma = 90°$) and the *C*2*mm* planar symmetry group.[11]

The Col3 phase and the rectangular *C*2*mm* symmetry are also found for all the compounds of the ***n*-234** series with the longest chains and for both compounds of the ***n*-23** series. For the organyl **10-234**, the X-ray pattern registered at 220 °C is compatible with rectangular *C*2*mm* symmetry. However, at lower temperatures, this symmetry breaks into the oblique *P*2 symmetry[12] ($\gamma \neq 90°$) (Col2 phase). In Table 2, the indexation is detailed at 120 °C for each palladium organyl exhibiting the Col2 or the Col3 phases.

The variation with temperature of the parameters *a* and *b* of the two-dimensional rectangular lattice in the Col3 phase (Fig. 2) is shown in Fig. 3(*a*) for the palladium organyl **12-234**: *b* increases while *a* decreases slowly with increasing temperature. This indicates that the mean stretching direction of the aliphatic tails is parallel to ***a***.[8] In Fig. 4, the experimental variation of *b* is compared to the value obtained from the experimental lattice area *s* and the molecular length *L* calculated by molecular modelling for the fully stretched conformation, and to the value obtained from *s* for a virtual hexagonal lattice [see Fig. 5 and eqn. (1a) and (1b)]. This comparison shows that in the Col3 phase the stretching of the aliphatic tails along ***a*** decreases with increasing chain length.

$$b'' = 3^{-1/2} a'' = 3^{-1/4} (ab)^{1/2} \quad (1a)$$

$$a' = 2L; \quad b' = \frac{ab}{2L} \quad (1b)$$

The variation with temperature of the lattice parameters in the Col2 phase of the homologue **10-234** is shown in Fig. 3(b). It is observed that, while *a* and γ increase with increasing temperature, *b* is almost independent of temperature. Moreover, this value of *b* is close to that determined for the **12-234** compound at low temperature. For further increases in chain lengths, larger values of *b* are obtained (see Fig. 4).

The value of *b* should be at a minimum when the intercalated segments are fully stretched along the longest side of the flat core. This is nearly the case for the homologues **10-234** and **12-234**. The minimum value of *b* found experimentally corresponds approximately to the transverse dimension of the flat core added to twice the diameter of a stretched and molten

Table 2 Detailed indexation at a given temperature of all liquid-crystalline phases of each palladium organyl [θ_{obs}, d_{obs}, θ_{calc}, d_{calc} are the diffraction angle (in degrees) and the corresponding spacing (in Å) which are observed (obs) and calculated (calc) respectively; I is the intensity of the diffraction signal; hk is the indexation of the two-dimensional lattice; a, b and γ are the lattice parameters; s is the lattice area]

6-234 (rectangular *C*2*mm*, 120 °C)

θ_{obs}	d_{obs}	I	hk	θ_{calc}	d_{calc}
1.49	29.6	VS	20	1.49	29.5
2.76	16.0	VS	11	2.76	16.0
2.99	14.76	S	40	2.99	14.76
3.49	12.6	VW	31	3.48	12.7
4.51	9.80	S	60	4.49	9.84
5.33	8.3	VW	02	5.32	8.30
5.54	8.0	VW	22	5.53	7.99
5.90	7.49	M	71	5.88	7.52
5.99	7.38	M	80	5.99	7.38
7.0	6.35	VW	62	6.97	6.35
7.25	6.10	W	91	7.25	6.10
8.0	5.50	VW	82	8.02	5.52
8.64	5.13	W	111	8.64	5.11
10.54	4.21	S			
12.8	3.48	W			

$a = 59.1$ Å, $b = 16.6$ Å, $\gamma = 90°$, $s = 981$ Å^2

8-234 (rectangular *C*2*mm*, 120 °C)

θ_{obs}	d_{obs}	I	hk	θ_{calc}	d_{calc}
1.33	33.3	VS	20	1.33	33.2
2.54	17.4	VS	11	2.54	17.4
2.66	16.6	M	40	2.66	16.6
3.15	14.00	M	31	3.16	13.99
3.98	11.09	S	60	3.99	11.07
4.12	10.73	W	51	4.13	10.70
5.11	8.7	VW	22	5.07	8.71
5.29	8.35	S	71	5.26	8.40
5.29	8.35	S	80	5.32	8.30
5.57	7.9	VW	42	5.57	7.93
6.48	6.83	W	91	6.48	6.83
7.27	6.1	VW	82	7.24	6.11
7.77	5.7	VW	111	7.74	5.72
8.39	5.28	W			
10.22	4.34	S			
12.3	3.63	W			

$a = 66.4$ Å, $b = 18.0$ Å, $\gamma = 90°$, $s = 1198$ Å^2

10-234 (oblique, 120 °C)

θ_{obs}	d_{obs}	I	hk	θ_{calc}	d_{calc}
1.41	31.4	VS	20	1.41	31.4
1.98	22.3	VS	11	1.98	22.3
2.28	19.4	VS	$\bar{1}1$	2.28	19.4
2.82	15.6	VW	40	2.82	15.7
3.23	13.68	S	$\bar{3}1$	3.22	13.69
3.65	12.10	M	51	3.66	12.05
4.01	11.01	S	22	3.97	11.13
4.01	11.01	S	02	4.03	10.95
4.23	10.4	VW	60	4.22	10.45
4.54	9.72	M	$\bar{2}2$	4.55	9.70
4.95	9.00	W	71	4.90	9.02
5.65	7.8	VW	80	5.64	7.84
6.39	6.92	W	$\bar{6}2$	6.45	6.85

$a = 64.3$ Å, $b = 22.5$ Å, $\gamma = 77.3°$, $s = 1409$ Å^2

12-234 (rectangular *C*2*mm*, 120 °C)

θ_{obs}	d_{obs}	I	hk	θ_{calc}	d_{calc}
1.23	35.8	VS	20	1.23	35.8
2.03	21.8	VS	11	2.03	21.8
2.68	16.5	M	31	2.68	16.5
3.69	11.96	W	51	3.64	12.13
3.69	11.96	W	60	3.70	11.93
3.84	11.50	M	02	3.87	11.42
4.04	10.93	W	22	4.06	10.88
4.70	9.40	W	71	4.74	9.33
4.98	9.0	VW	80	4.94	8.95

$a = 71.6$ Å, $b = 22.8$ Å, $\gamma = 90°$, $s = 1635$ Å^2

14-234 (rectangular *C*2*mm*, 120 °C)

θ_{obs}	d_{obs}	I	hk	θ_{calc}	d_{calc}
1.20	36.8	VS	20	1.20	36.8
1.87	23.6	VS	11	1.87	23.6
2.39	18.5	VW	40	2.40	18.4
2.54	17.4	M	31	2.52	17.5
3.51	12.6	M	02	3.48	12.48
3.51	12.6	M	51	3.54	12.68
3.72	11.86	W	22	3.74	11.82

$a = 73.6$ Å, $b = 25.0$ Å, $\gamma = 90°$, $s = 1837$ Å^2

14-234 (rectangular *P*2*gg*, 200 °C)

θ_{obs}	d_{obs}	I	hk	θ_{calc}	d_{calc}
1.42	31.0	VS	11	1.42	31.0
1.66	26.6	VS	20	1.66	26.6
2.03	21.8	S	21	2.02	21.8
2.31	19.1	VW	02	2.31	19.1
2.47	17.9	VW	12	2.46	18.0
2.75	16.0	M	31	2.75	16.1
3.42	12.90	M	32	3.40	12.99
3.86	11.45	W	23	3.85	11.47

$a = 53.2$ Å, $b = 38.2$ Å, $\gamma = 90°$, $s = 2029$ Å^2

16-234 (rectangular *C*2*mm*, 120 °C)

θ_{obs}	d_{obs}	I	hk	θ_{calc}	d_{calc}
1.16	37.9	VS	20	1.16	37.9
1.74	25.4	VS	11	1.74	25.4
2.41	18.3	M	31	2.40	18.4
3.29	13.4	S	02	3.28	13.45
3.29	13.4	S	51	3.34	13.21
3.50	12.6	S	22	3.48	12.68
3.50	12.6	S	62	3.49	12.64
4.37	10.1	VW	71	4.40	10.05
4.65	9.5	VW	80	4.66	9.48

$a = 75.8$ Å, $b = 26.9$ Å, $\gamma = 90°$, $s = 2040$ Å^2

18-234 (rectangular *C*2*mm*, 120 °C)

θ_{obs}	d_{obs}	I	hk	θ_{calc}	d_{calc}
1.11	39.7	VS	20	1.11	39.7
1.63	27.1	VS	11	1.63	27.1
2.26	19.5	M	31	2.27	19.5
3.07	14.38	S	02	3.06	14.41
3.26	13.53	M	22	3.26	13.54
3.34	13.2	VW	60	3.34	13.22
4.21	10.50	W	71	4.19	10.55
4.53	9.75	W	62	4.54	9.74

$a = 79.3$ Å, $b = 28.8$ Å, $\gamma = 90°$, $s = 2287$ Å^2

18-234 (rectangular *P*2*gg*, 200 °C)

θ_{obs}	d_{obs}	I	hk	θ_{calc}	d_{calc}
1.29	34.3	11	VS	1.29	34.3
1.48	29.9	20	VS	1.48	29.9
1.81	24.3	21	S	1.81	24.4
2.10	21.0	02	W	2.10	21.0
2.46	18.0	31	M	2.45	18.0

$a = 59.8$ Å, $b = 41.9$ Å, $\gamma = 90°$, $s = 2509$ Å^2

12-24 (rectangular *C*2*mm*, 120 °C)

θ_{obs}	d_{obs}	I	hk	θ_{calc}	d_{calc}
1.35	32.6	VS	20	1.35	32.6
2.64	16.7	VS	11	2.64	16.7
3.25	13.59	W	31	3.26	13.54
4.07	10.85	M	60	4.06	10.87
5.26	8.40	M	22	5.29	8.36
5.44	8.13	M	71	5.39	8.20
5.44	8.13	M	80	5.42	8.15
6.60	6.70	W	62	6.60	6.70
10.94	4.06	S			
13.13	3.39	W			

$a = 65.3$ Å, $b = 17.3$ Å, $\gamma = 90°$, $s = 1129$ Å^2

12-23 (rectangular *C*2*mm*, 120 °C)

θ_{obs}	d_{obs}	I	hk	θ_{calc}	d_{calc}
1.69	26.2	VS	20	1.69	26.2
2.13	20.8	VS	11	2.13	20.8
3.38	13.07	S	40	3.38	13.08
3.90	11.32	W	02	3.91	11.30
4.3	10.4	VW	22	4.26	10.37
4.64	9.52	M	51	4.65	9.50
5.07	8.69	M	60	5.09	8.72
6.23	7.10	W	71	6.23	7.10
6.8	6.5	VW	80	6.76	6.54

$a = 52.4$ Å, $b = 22.6$ Å, $\gamma = 90°$, $s = 1183$ Å^2

12-23 (rectangular *P*2*gg*, 180 °C)

θ_{obs}	d_{obs}	I	hk	θ_{calc}	d_{calc}
1.83	24.1	VS	11	1.83	24.1
2.09	21.1	S	20	2.09	21.1
2.57	17.1	S	21	2.57	17.1
3.02	14.64	W	02	2.98	14.68
3.17	13.95	S	12	3.18	13.87
3.5	12.7	VW	31	3.47	12.70
4.35	10.16	S	32	4.35	10.16
4.4	10.0	VW	41	4.44	9.94
4.97	8.89	M	23	4.98	8.88

$a = 42.3$ Å, $b = 29.4$ Å, $\gamma = 90°$, $s = 1241$ Å^2

Table 2—Continued

18-23 (rectangular *C*2*mm*, 120 °C)						**18-23** (rectangular *P*2*gg*, 180 °C)					
θ_{obs}	d_{obs}	*I*	*hk*	θ_{calc}	d_{calc}	θ_{obs}	d_{obs}	*I*	*hk*	θ_{calc}	d_{calc}
1.54	28.6	S	20	1.54	28.6	1.60	27.5	VS	11	1.60	27.5
1.73	25.5	VS	11	1.73	25.5	1.69	26.1	S	20	1.69	26.1
2.78	15.8	W	31	2.78	15.8	2.17	20.4	M	21	2.17	20.3
3.09	14.3	M	40	3.09	14.29	2.72	16.2	W	02	2.72	16.2
3.09	14.3	M	02	3.10	14.26	2.87	15.4	M	12	2.85	15.48
3.46	12.77	M	22	3.46	12.76	2.87	15.4	M	31	2.88	15.34
4.14	10.67	W	51	4.16	10.61	3.22	13.7	VW	22	3.20	13.78
4.63	9.54	W	60	4.64	9.53	3.40	13.0	VW	40	3.38	13.06
5.59	7.9	VW	71	5.63	7.85	3.70	11.93	M	41	3.65	12.11
						3.70	11.93	M	32	3.72	11.87
$a=57.2$ Å				$\gamma=90°$		$a=52.2$ Å				$\gamma=90°$	
$b=28.5$ Å				$s=1630$ Å^2		$b=32.4$ Å				$s=1694$ Å^2	

VS: very strong; S: strong; M: medium; W: weak; VW: very weak.

aliphatic chain.[12] For longer chain lengths, these segments may coil, consistent with the larger *b* values observed, while for smaller chain lengths the organyls exhibit the ordered columnar phase Col1. The results obtained for both compounds of the ***n*-23** palladium organyl series confirm that the ratio between the longest side of the flat core and the chain length determines the spacing within the rows and therefore the whole packing geometry. Let us recall that the rows are defined parallel to the *b* axis and that the chains are attached to the short side of the columnar cores. In fact, these chains are folded and sandwiched between the long sides of the columnar cores within the rows.

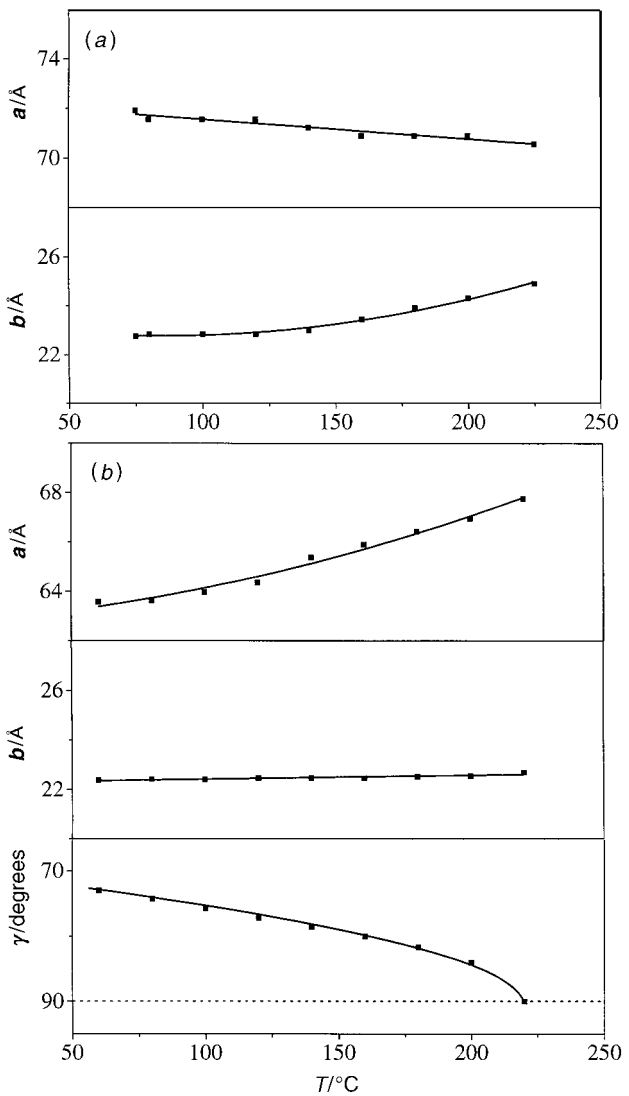

Fig. 3 Variation as a function of temperature of the lattice parameters *a*, *b* and γ: (*a*) Col3 phase of the palladium organyl **12-234** ($\gamma=90°$); (*b*) Col2 phase of the palladium organyl **10-234**

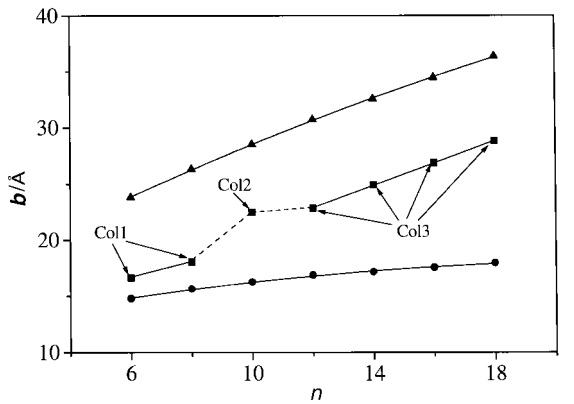

Fig. 4 Variation of the lattice parameter *b* at 120 °C as a function of *n* for the ***n*-234** palladium organyl series (■) and comparison to the theoretical variations for the virtual 'fully stretched' (●) and 'hexagonal' (▲) lattices with the same area (see text)

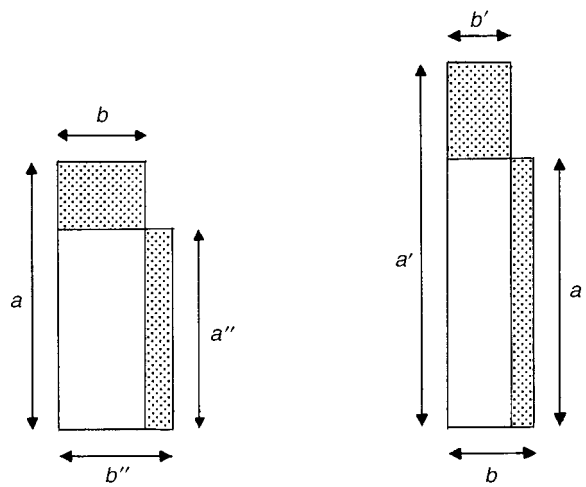

Fig. 5 Comparison of the real rectangular lattice to the virtual 'fully stretched' and 'hexagonal' lattices with the same area. Using eqn. (1a), (1b) and (1c), the parameter β_1 is calculated from the intersection areas of the real and virtual lattices. This parameter is equal to 0 for the 'fully stretched' lattice and 1 for the 'hexagonal' lattice (see text).

Indeed, the same value of b is found for the homologues **12-23** and **18-234**, and for the longer ones **18-234** and **18-234** [despite the very different lattice areas and the difference between the bulkiness of the chains (see Table 2)]. This suggests the schematic view that the chains in position **2** are intercalated and those in positions **3** and **4** are rejected out of the rows.

There is an influence of temperature on the difference between the length of intercalated chain segments and that of flat core sides. Thus, the increase of b at high temperature for the palladium organyl **12-234** reveals an increasing coiling with increasing temperature. For the compound **10-234**, the tilt angle between the flat core long sides and the row normal $(\pi/2-\gamma)$ (see Fig. 6) decreases with increasing temperature. Both these results suggest that the intercalated segments become longer with increasing temperature.

For the compound **10-234** at low temperature, the intercalated segments are shorter than the long flat core sides and the discrepancy is compensated by the tilting. For the compound **12-234** at high temperature, the intercalated segments are longer than the long flat core sides, and these segments can therefore coil. The origin of such a temperature dependence can be related to the fact that the chains are connected to the short flat core side and have to form loops to intercalate. Thus, with increasing temperature, the loops can be constituted by shorter chain segments due to a greater mobility of the chains.

With increasing chain length, b increases and the coiling of the intercalated segments is more important. In parallel, a increases and the aliphatic density located between the rows is larger. The parameter β_1 compares the real lattice to virtual lattices of the same area corresponding to the fully stretched molecular conformation and to the hexagonal packing [see Fig. 5 and the eqn. (1a)–(1c)].

$$\beta_1 = \frac{\left(1-\frac{b'}{b}\right)}{\left(1-\frac{b'}{b''}\right)} \qquad (1c)$$

β_1 varies between 0 and 1 for the 'fully stretched' and the 'hexagonal' packings, respectively. The experimental variation of β_1 for the homologues **10-234** to **18-234** [see Fig. 7(*a*)] clearly indicates that the variation of b prevails over that of a.

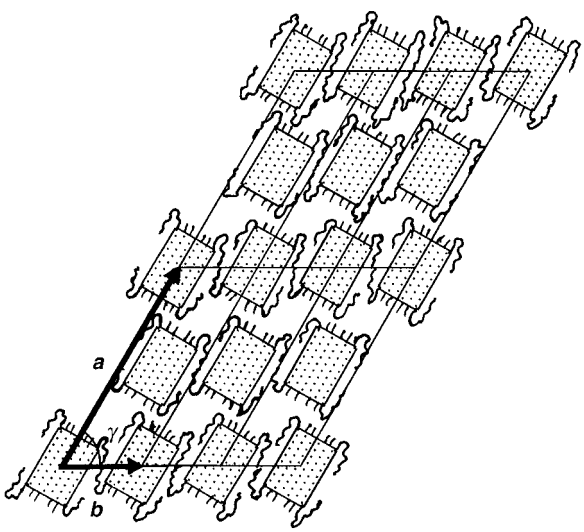

Fig. 6 Packing model within the Col2 phase. The discrepancy between the lengths of the flat core side and of the intercalated chain segments occurring for the palladium organyl **10-234** is compensated by the tilt angle within the rows. For the sake of clarity, only the beginnings of the chains rejected out of the rows (8 over 12) is represented.

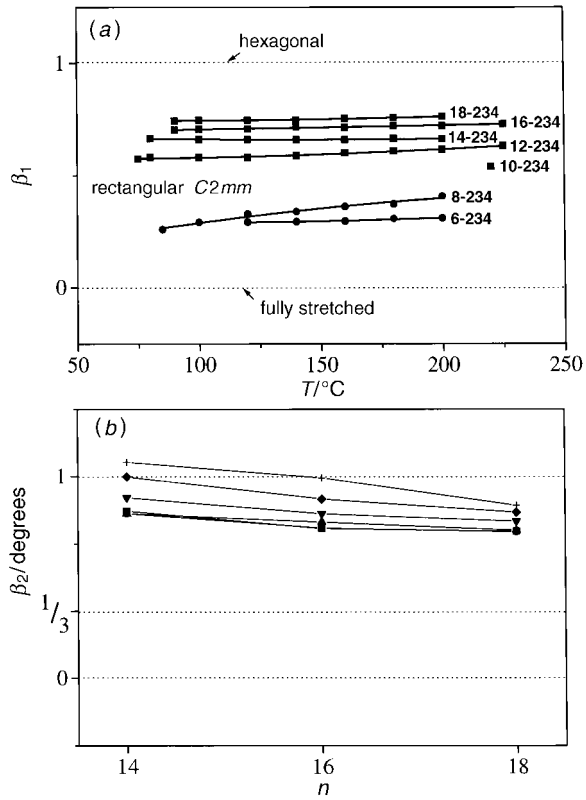

Fig. 7 Variation of the parameter β_1 as a function of chain length and temperature, in the ***n*-234** palladium organyl series: (*a*) for the phases Col1 (●) and Col3 (■); (*b*) of the parameter β_2, for the phase Col3 at 100 °C (■), 120 °C (●), 140 °C (▲), 160 °C (▼), 180 °C (◆) and 200 °C (+).

With increasing chain length, the thickness of the aliphatic crown becomes more and more homogeneous. Consequently, the packing geometry evolves towards the hexagonal symmetry, but this evolution slows for large chain lengths. In addition, increasing the temperature, like increasing the chain length, induces an increase of β_1, although the effect is smaller. This is consistent with the loop model developed above for the **10-234** and **12-234** homologues. As a matter of fact, the formation of the loops is easier and the chain segments involved in the loops are shorter, implying a larger coiling of the intercalated aliphatic segments and a larger spacing within the rows. With the assumption that the value of b (about 22.7 Å) found for the **10-234**, **12-234** and **12-23** compounds in the Col3 phase really corresponds to completely stretched intercalated segments, a parameter β_2 simulating the distribution of the additional area for the members **14-234**, **16-234** and **18-234** of the first series of palladium organyls [see Fig. 8 and eqn. (2a)–(2c)] can be calculated.

$$s_1 = a(b'-b) \qquad (2a)$$

$$s_2 = b(a'-a) \qquad (2b)$$

$$\beta_2 = \frac{s_1}{s_1+s_2} \qquad (2c)$$

β_2 would be equal to 0 if the additional area were located out of the rows, equal to 1 for a complete location within the rows, and equal to 1/3 for a balanced distribution. The experimental β_2 variation [see Fig. 7(*b*)] shows that the additional area is mainly located within the rows, by the coiling of the intercalated segments. However, the small fraction located out of the rows seems to increase with chain length (maybe a more favourable degree of coiling is then reached?). The expansion of β_2 and of the fraction located within the rows with increasing

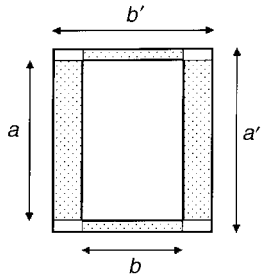

Fig. 8 Distribution of the additional area for the palladium organyls **14-234**, **16-234** and **18-234** with respect to the homologues **10-234** and **12-234**, in the Col3 phase. Using eqn. (2a), (2b) and (2c), the parameter β_2 is calculated from the variation of the lattice parameters a and b. β_2 would be equal to 0 if the additional area were located out of the rows, equal to 1 if the additional area were located within the rows and equal to 1/3 for a balanced distribution.

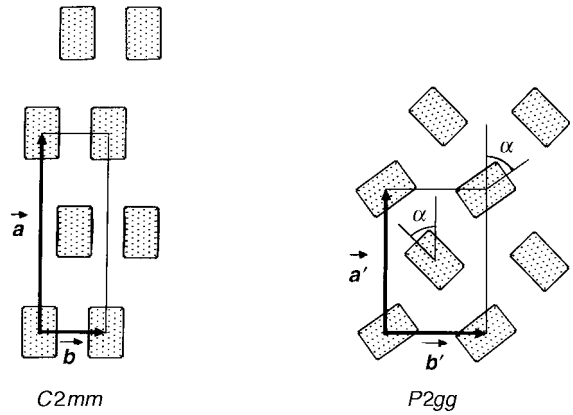

Fig. 9 Comparison of the structures proposed for the Col3 phase (rectangular *C2mm*) and the Col4 phase (rectangular *P2gg*). The mean tilt angle α is evaluated from the lattice parameters ratio in both phases using eqn. (3a) and (3b) (see text).

temperature is consistent with the loop model. However, the effect becomes important only above 150 °C.

(b) *The phase Col4*. For the long chain derivatives ($n \geqslant 14$), an irreversible transition of the Col3 phase into the Col4 phase takes place above 140 °C. This transformation is complete for the **18-23** compound, but not complete for the other derivatives for which a mixture of both Col3 and Col4 phases is always observed. The very slow kinetics of the transformation indicates that the packings within the Col3 and Col4 phases have similar energies. The irreversible character of this transformation for the longest chain derivative seems to indicate, however, that the Col4 phase is more stable. The transformation may be related to a decomposition process. Although this hypothesis cannot be completely ruled out, there are strong arguments against such an interpretation. First, the lattices within the Col3 and Col4 phases (see below) have almost the same area, in agreement with the assumption that the transformation between them preserves the columnar core and the columnar periphery, with the orientation of the columnar cores within the lattice being only slightly changed. Second, further experiments have been performed on mixtures of **12-234** with a few percent of pentadecane in order to confirm that the Col4 phase is a stable mesophase observed for the long aliphatic chain derivatives. In this case, the Col4 phase was unambiguously the only one observed within the whole mesomorphic domain. While for the long chain derivatives, the occurrence of the Col4 phase is obviously related to the aliphatic chain length, in the case of mixtures it results from the swelling of the aliphatic periphery. Both cases show the importance of the amount of aliphatic medium on the generation of the Col4 phase.

Let us now describe in detail the structure of the Col4 phase. In this phase, the lattice is rectangular and the area is the same as in the Col3 phase, but with very different lattice parameters (see Table 3). In addition, the lattice is not centred any more, since the reflections extinguished in the *C2mm* plane symmetry group ($h+k=2n+1$) are visible in the X-ray patterns (the reflections $h0$ and $0k$ with $h,k=2n+1$ remain extinguished; see Table 2). Both this result and the evolution of the lattice parameter ratio (a/b) between both phases, without significant change of the lattice area (see Fig. 10), suggest that the flat cores are tilted with respect to ***a***, but with a change of their orientation from row to row. This corresponds to the *P2gg* plane symmetry group[11] (Fig. 9). By neglecting the changes in the packing of the aliphatic tails, the mean tilt angle α in the Col4 phase was evaluated from the lattice parameter ratios in both phases, by using eqn. (3a) and (3b). For a particular angle α_{hex} [given by eqn. (3c)], the ratio a'/b' is equal to $\sqrt{3}$ and the lattice is pseudo-hexagonal. In all cases, the experimental ratios are slightly smaller and the experimental tilt angles slightly larger than these particular values (see Fig. 10 and Table 3).

$$b' = \frac{b}{\cos\alpha}; \quad a' = a\cos\alpha \tag{3a}$$

$$\alpha = \arccos\sqrt{\left(\frac{a'}{b'}\frac{b}{a}\right)} \tag{3b}$$

$$\alpha_{hex} = \arccos\sqrt{\left(\sqrt{3}\,\frac{b}{a}\right)} \tag{3c}$$

The ordered columnar phase Col1. Both members of the ***n*-234** series with n smaller than 10, as well as the organyl **12-24**, show the 'ordered' columnar phase Col1. The structure of this phase is similar to that of the Col3 phase. The columns are arranged in a rectangular centred lattice, according to the *C2mm* plane symmetry group (see Fig. 2). However, the tough pasty consistency of the samples, as well as some features of the patterns, suggest that the positions of the flat cores are long-range correlated (in the disordered columnar phases, only the positions of the columns are long-range correlated). Thus,

Table 3 Comparison of the lattice parameters in the Col3 and Col4 phases for several compounds of the ***n*-234** and ***n*-23** palladium organyl series ($ab^{-1}-3^{0.5}$ represents the deviation from the hexagonal lattice; α is the mean tilt angle in the Col4 phase)

				Col3				Col4			
mesogen	T/°C	s^a/Å^2	$\alpha_{hex}{}^b$/degrees	a/Å	b/Å	$ab^{-1}-3^{0.5}$	α/degrees	a/Å	b/Å	$ab^{-1}-3^{0.5}$	α/degrees
14-234	200	2012	38.5	75.1	26.6	1.10	0	53.2	38.2	−0.34	45.4
18-234	200	2513	35.0	80.6	31.2	0.85	0	59.8	41.9	−0.31	42.0
12-23	180	1246	31.6	54.7	22.9	0.66	0	42.3	29.4	−0.29	39.1
18-23	180	1717	25.1	60.6	28.7	0.38	0	52.2	32.4	−0.12	29.1

[a]Mean value of the unit cell area for both rectangular phases at the temperature T. [b]Theoretical chevron tilt angle toward ***a*** for hexagonal packing (see text).

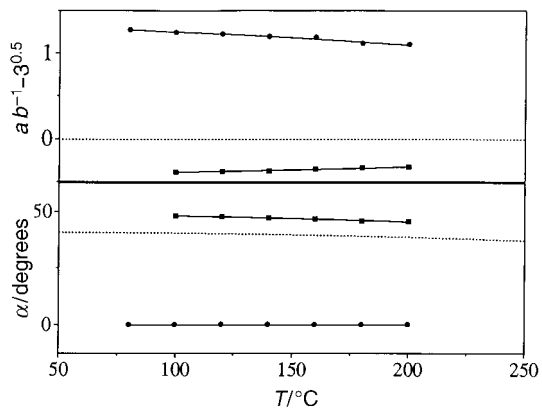

Fig. 10 Shift from the hexagonal geometry and mean tilt angle α as a function of temperature in the Col3 phase (●) and in the Col4 phase (■), for the palladium organyl **14-234**. The dotted line corresponds to the virtual hexagonal lattice with the same area.

the decrease of the intensity of the *hk*0 reflections with increasing Bragg angle is much smaller than in the case of the Col3 and Col2 phases. There are also some sharp reflections in the wide-angle region belonging to other families of planes (see Table 2). Nevertheless, the Col1 phase has to be considered as a liquid-crystalline like phase in view of the presence of a diffuse reflection at about 4.5 Å which indicates that the aliphatic chains are molten. This is confirmed by the variation of the lattice area as a function of chain length which has been found linear whatever the columnar phase (see Fig. 12 below).

It is observed that the lattice parameter *b* in the Col1 phase is only about 17.5 Å at 120 °C (see Table 2), corresponding to the transverse dimension of the flat core plus one diameter of a stretched aliphatic chain[12] (instead of the two diameters needed in the Col2 and Col3 phases); therefore, the half number of the intercalated chain segments in the disordered phases are rejected out of the rows. This is confirmed by the very similar *b* value determined for both members, **6-234** and **8-234** and for the organyl **12-24** [despite the very different lattice areas and the differences between the bulkiness of chains (see Table 2)]. These results clearly indicate that the occurrence of the long-range correlations is related to the smaller spacing within the rows.

For the two homologues **8-234** and **6-234**, the side length of the flat cores is larger than the total length of the intercalated segments. In the Col3 phase of the **10-234** compound of this series, the small difference is compensated by the tilting of the flat cores within the rows (see the section on the phases Col2 and Col3). In contrast, in the Col1 phase there is no tilting to compensate the discrepancy between the lengths, even if the β_1 variation for the homologue **8-234** {but not for the still lower one, **6-234** [see Fig. 7(*a*)]} reveals the coiling of the intercalated chains at high temperature. This strongly suggests that there is an alternative mechanism of compensation related to the packing within the columns (see next section).

Packing within the columns

As well as in the disordered columnar phases Col2, Col3 and Col4, in the ordered columnar phase Col1 the mean orientation of the flat cores in the columnar section is the same all along the column. If not, the lattice geometry would not reproduce the anisotropy of the flat core structure and the symmetry would be hexagonal. It happens that, within a column, the mean positions of stacked neighbouring flat cores can either be aligned to the normal of the flat core planes or be laterally shifted with respect to it. In the first case [Fig. 11(*a*)], the angle between the mean columnar axis and the normal of the flat core planes is zero, corresponding to an 'untilted' columnar

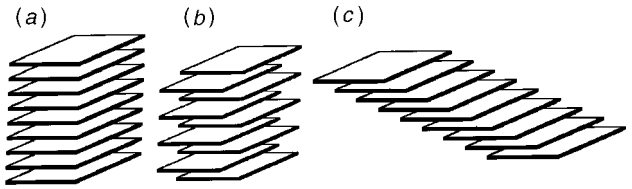

Fig. 11 Types of packing within the columns considered in the analysis of the columnar structure of the palladium organyls: (*a*) true untilted packing, (*b*) apparent untilted packing, with the flat core positions shifted from the columnar axis, but with periodical changes in the shift direction averaging the tilt angle to zero, (*c*) tilted packing, corresponding to a unique or a preferential shift direction.

phase. In the second case, the columnar phase is also 'untilted', if periodical changes in the shift direction average the tilt angle to zero [Fig. 11(*b*)]. Alternatively, the columnar phase is 'tilted', if there is one unique or a preferential lateral shift direction [Fig. 11(*c*)]. From the analysis of the lattice area and stacking period values and variations, no distinction can be made between the two kinds of untilted phases. However, the presence of the tilt angle gives a smaller lattice area and a larger stacking period for the 'tilted' phase.

Indeed, the variation of the lattice area as a function of chain length is linear (see Fig. 12). This indicates that the tilt angle has the same value in all phases, for all organyls. This value can be obtained from the extrapolation to zero chain length of the lattice area which can be compared to the flat core area. Unfortunately, the difference between the columnar core area (165 Å^2) and the flat core area (about 160 Å^2 when taking into account the real 'knucklebone' shape of the molecule) is not significant. Therefore a zero or a non-zero tilt angle could not be distinguished. From the slope of the lattice area variation as a function of chain length and from the volume of the aliphatic chains,[12] the columnar stacking period *h* could be deduced. The resulting value, 6.45 Å at 120 °C, is comparable to the ratio of the molecular volume (obtained by dilatometry) and of the lattice area (6.4 $\pm$ 0.1 Å in the range 70–220 °C, for the palladium organyl **12-234**). The agreement between these values confirms that the tilt angle is the same for the flat cores and for the aliphatic crown, whether its value is zero or non-zero. Moreover, the stacking period and the zero or non-zero tilt angle show no significant dependence upon temperature.

Previously, very similar values and temperature dependences were found for the stacking period and lattice parameters of a tetraplatinum organyl which is similar to the tetrapalladium one **12-234** (for the rectangular *C*2*mm* cell at 120 °C: $a = 71.8$ Å, $b = 23.4$ Å, $s = 1680$ Å^2, $h = 6.31$ Å[8]). As the platinum and

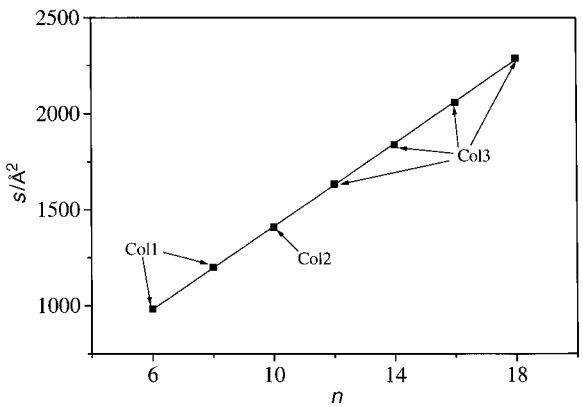

Fig. 12 Variation of the lattice area as a function of chain length at 120 °C, for the ***n*-234** palladium organyl series, within the Col1, Col2 and Col3 phases

palladium complexes have the same geometry, both organyls show the same type of liquid-crystalline organisation and similar packing parameters. In contrast, in the crystalline phase of the analogue to the **6-234** organyl (with iodide instead of chloride bridges[7]), the columnar organisation is similar to that of the Col1, Col2 and Col3 phases, but with a larger stacking period (8.6 Å) and a smaller area of the columnar section (370 $Å^2$ instead of 490 $Å^2$). Such a large discrepancy cannot be explained by the greater bulk of the iodide ions and by the probably different mean conformation of the phenylene diamine rings. Instead it can be explained by the state of the aliphatic chains, 'crystallised' and stiff in one case, and 'molten' and flexible in the other case. This is confirmed by the fact that in spite of the long-range correlated core positions (but molten aliphatic chains) the columnar section and the stacking period are the same in the Col1 phase and in the Col2 to Col4 phases.

No definitive statement on the tilted or untilted nature of the phases Col1 to Col4 can be made from the discussion above. Nevertheless, the result that the zero or non-zero tilt angle value is the same for all phases, chain lengths and temperatures makes the untilted case seem more probable. In addition, a nearly zero tilt angle is found in the crystalline phase of the iodide-bridged **6-234** organyl analogue. In that case, the stacking period is larger than that found in Col1 to Col4 phases. A tilted columnar phase was generated by replacing the linear chains by branched ones.[13] This resulted in a large decrease of the lattice area and of the a/b ratio, which contributed to a large increase of the stacking period. In the Col1 to Col4 phases the flat core and columnar core areas were similar and the a/b ratios were compatible with the molecular dimensions, implying that the tilt angle was zero or small.

Let us now consider the occurrence of periodical shifts from the main columnar axis [see Fig. 11(*b*)]. In this case, the positions of neighbouring flat cores are shifted in opposite directions as in the case of the crystalline phase of the iodide-bridged **6-234** organyl analogue.[7] In the Col1 phase of **6-234**, we can assume that a periodic shift along a probably exists since the length of two stretched hexyloxy tails is smaller than the side length of the flat cores, which are separated by the thickness of one chain (see the section on the ordered columnar phase Col1). In the case of its homologue, **8-234**, there is a smaller discrepancy which could be compensated by a smaller shift. However, this organyl shows slightly larger values of b and β_1 which increase with temperature. This reveals the coiling of the intercalated chains and implies that the shift is larger than the minimum value. The occurrence of such a periodical shift in the disordered columnar phases is possible, but rather unlikely. Thus, the small discrepancy remaining in the case of the organyl **10-234** is compensated by a lateral shift in the position of the columns. Then, the intercalated segments are stretched for its higher homologue **12-234** and further increasing chain length results in the corresponding increase of b (see the section on the phases Col2 and Col3).

Conclusion

The length of the twelve chains grafted to a tetrapalladium organyl based flat core was varied between six and eighteen carbons, by steps of two. In addition, three organyls with the same flat core, but only eight chains, were also synthesised. These ten compounds show columnar phases with a long-range ordered two-dimensional lattice of *C*2*mm* symmetry. A Col1 phase is observed for the short chain compounds, and a Col3 phase for the long chain compounds. Between these two rectangular centred phases, another columnar phase, Col2, exists for the representative **10-234** compound which exhibits this phase below 220 °C. The Col2 phase consists of a two-dimensional columnar arrangement with *P*2 symmetry, whereby the opening angle of the oblique lattice increases continuously with temperature, becoming equal to 90° at the Col2–Col3 phase transition. In the Col3 phase, the columns are arranged in stacked rows with one chain out of three intercalated between the flat molecular cores which are equally oriented with the long side normal to the row. The evolution of the lattice parameters with chain length and temperature is explained by the length and the coiling of the intercalated chains. For the **10-234** compound, the length of the intercalated chains becomes shorter than the length of the longer sides of the flat rectangular cores of the molecules. This mismatch is compensated by the tilting of the flat cores within the rows. The organyls which exhibit the Col1 phase have shorter chains but the flat cores are not tilted within the rows. This larger discrepancy could be compensated by periodical shifts of the columnar axis within the columns. Unlike the case of the other Col2 and Col3 columnar phases, only one chain out of six is intercalated in the Col1 phase and there are long-range correlations in the positions of the flat cores within the columns. At high temperature, the homologues with the longest chains present a very slow transition from the Col3 to the Col4 phase, and the flat cores are tilted in opposite directions on two successive rows (*P*2*gg* symmetry). No definitive statement can be made about the occurrence of a non-zero tilt angle between the normal to the plane containing the flat cores and the columnar axis. However, we have shown that this non-zero value would be small and identical for all phases and metal organyls presented here, and that the planes containing the flat cores and the chains must be the same. This makes the zero-tilt angle alternative more likely.

Experimental

The transition temperatures were determined by DSC using a Mettler TA 3000 with TA 72.5 software. The X-ray diffraction patterns were obtained with two different experimental setups, the crude powder being in all cases filled in Lindemann capillaries. The measurements were performed by using a linear monochromatic Cu-Kα_1 beam obtained with a sealed-tube generator and a bent quartz monochromator. The diffraction patterns were registered on films. The temperatures of the samples were controlled within ± 0.3 °C. For weak or diffuse reflections, a linear monochromatic Cu-Kα_1 beam obtained with a sealed-tube generator and a bent quartz monochromator was used together with a curved counter Inel CPS 120. For this setup the temperatures of the samples were controlled within ± 0.05 °C. Dilatometric measurements were performed with a high-precision home-built apparatus with automatic computer-controlled operation, including data acquisition and temperature control within ± 0.03 °C.[14] With this equipment a resolution of 10^{-2}% was obtained with respect to the relative variations of the specific volume and an accuracy of 10^{-1}% for the absolute value.

The members of the ***n*-234** palladium organyl series were obtained from the benzal derivatives from 1,4-diaminobenzene and 3,4,5-trialkyloxybenzaldehyde. The other palladium organyls (**12-23**, **18-23** and **12-24**) were obtained by the same synthetic route from 2,3- and 2,4-dialkyloxybenzaldehyde.

The syntheses of 2,3,4-trialkyloxybenzaldehydes were carried out by etherification of pyrogallol with the corresponding alkyl bromide in refluxing DMF and subsequent Vilsmeyer formylation, as described previously.[6,10] Alternately, the triethers were obtained in one step from commercially available 2,3,4-trihydroxybenzaldehyde, following the same standard procedure, which was also the one used to prepare dialkyloxybenzaldehydes from the corresponding commercial dihydroxybenzaldehydes. Overall yields were between 20 and 40% for the two-step reaction and between 80 and 90% for the one-step reaction. 2,3,4-Trialkyloxybenzaldehydes (alkyl = hexyl): yellowish oil (impure), $C_{25}H_{42}O_4$ (406.6); alkyl = octyl:

colourless oil, $C_{31}H_{54}O_4$ (490.8); alkyl = decyl,[10] alkyl = dodecyl,[6] alkyl = tetradecyl,[10] alkyl = hexadecyl: colourless powder, $C_{55}H_{102}O_4$ (827.4); alkyl = octadecyl: colourless powder, $C_{61}H_{114}O_4$ (911.6); identical ^{1}H NMR data.[6,10] 2,3-Dialkyloxybenzaldehydes: alkyl = dodecyl: colourless powder, mp 48 °C, $C_{31}H_{54}O_3$ (474.8); alkyl = octadecyl: colourless powder, mp 74 °C, $C_{43}H_{78}O_3$ (643.1); identical ^{1}H NMR data ($CDCl_3$): $\delta = 10.05$ (s, C*H*O), 7.40, 7.12, 7.09 (3 dd, $^3J = 8$ Hz, $^4J = 2$ Hz, aromatic H), 4.13, 4.00 (2t, $J = 7$ Hz, OCH_2), 1.88–1.75 (m, OCH_2CH_2), 1.54–1.41 (m, $OCH_2CH_2CH_2$), 1.40–1.20 (m, further CH_2 groups), 0.89 (t, $J = 7$ Hz, CH_3). 2,4-Didodecyloxybenzaldehyde: colourless powder, mp 51 °C, $C_{31}H_{54}O_3$ (474.8); ^{1}H NMR ($CDCl_3$): $\delta = 10.33$ (s, C*H*O), 7.80 (d, $J = 8$ Hz), 7.62 (dd, $^3J = 8$ Hz, $^4J = 2$ Hz), 7.09 (d, $J = 2$ Hz, aromatic H), 4.03, 4.01 (2t, $J = 7$ Hz, OCH_2), 1.84, 1.79 (2tt, $J = 7$ Hz, OCH_2CH_2), 1.54–1.40 (m, $OCH_2CH_2CH_2$), 1.40–1.20 (m, further CH_2 groups), 0.88 (t, $J = 7$ Hz, CH_3).

The ligands 1,4-benzenebis(2,3,4-trialkyloxybenzal)imines and 1,4-benzenebis(dialkyloxybenzal)imines were obtained by condensation of the benzaldehyde derivatives and of 1,4-phenylenediamine in presence of toluene-*p*-sulfonic acid, as described elsewhere.[6,10] Yields between 50 and 90%. 1,4-Benzenebis(2,3,4-trialkyloxybenzal)imines: alkyl = hexyl: yellow powder, $C_{56}H_{88}O_6N_2$ (885.3); alkyl = octyl: yellow powder, $C_{68}H_{112}O_6N_2$ (1053.6); alkyl = decyl,[10] alkyl = dodecyl,[6] alkyl = tetradecyl,[10] alkyl = hexadecyl: yellow powder, $C_{116}H_{208}O_6N_2$ (1726.4); alkyl = octadecyl: yellow powder, $C_{128}H_{232}O_6N_2$ (1895.3); identical ^{1}H NMR data;[6,10] also nearly identical ^{13}C NMR data.[6,10] 1,4-Benzenebis(2,3-dialkyloxybenzal)imines: alkyl = octadecyl: yellow powder, mp 102 °C, $C_{92}H_{160}O_4N_2$ (1358.3); alkyl = dodecyl: yellow powder, mp 93 °C, $C_{68}H_{112}O_4N_2$ (1021.6); identical ^{1}H NMR data ($CDCl_3$): $\delta = 8.94$ (s, C*H*N), 7.74, 7.12, 7.01 (3dd, $^3J = 8$ Hz, $^4J = 2$ Hz, 2 aromatic H each), 7.24 (s, 4 aromatic H), 4.08, 4.01 (2t, $J = 7$ Hz, OCH_2), 1.88–1.75 (m, OCH_2CH_2), 1.54–1.41 (m, $OCH_2CH_2CH_2$), 1.40–1.20 (m, further CH_2 groups), 0.89 (t, $J = 7$ Hz, CH_3); ^{13}C NMR data ($CDCl_3$): $\delta = 155.94$ (d, 2 *C*HN groups), 152.55, 150.61, 149.99, 130.52 (4s, 2 aromatic C each), 123.77, 119.23, 116.49 (3d, 2 aromatic C each), 121.89 (d, 4 aromatic C), 69.20 (t, 4 OCH_2 groups), 31.93–29.34 (6t, 32 CH_2 groups), 26.24 (t, 4 CH_2 groups), 22.65 (t, 4 CH_2 groups), 13.98 (q, 4 CH_3 groups). 1,4-Benzenebis(2,4-didodecyloxybenzal)imine: yellow powder, mp 73 °C, $C_{68}H_{112}O_4N_2$ (1053.6); ^{1}H NMR data ($CDCl_3$): $\delta = 8.87$ (s, C*H*N), 8.09 (d, $J = 8$ Hz), 6.56 (dd, $^3J = 8$ Hz, $^4J = 2$ Hz), 6.45 (d, $J = 2$ Hz, 2 aromatic H each), 7.24 (s, 4 aromatic H), 4.02, 4.01 (2t, $J = 7$ Hz, OCH_2), 1.87–1.75 (m, OCH_2CH_2), 1.54–1.40 (m, $OCH_2CH_2CH_2$), 1.40–1.20 (m, further CH_2 groups), 0.88, 0.86 (2t, $J = 7$ Hz, CH_3); ^{13}C NMR data ($CDCl_3$): $\delta = 155.02$ (d, 2 *C*HN groups), 163.13, 160.42, 150.46, 118.26 (4s, 2 aromatic C each), 128.70, 106.10, 99.18 (3d, 2 aromatic C each), 121.77 (d, 4 aromatic C), 68.41, 68.15 (2t, 2 OCH_2 groups each), 31.88–29.09 (8t, 32 CH_2 groups), 26.08, 25.99 (2t, 2 CH_2 groups each), 22.65 (t, 4 CH_2 groups), 14.07 (q, 4 CH_3 groups).

The members of the ***n*-234** palladium organyl series (tetra-μ-chlorobis{μ-[1,4-phenylenebis(nitrilomethylidene-3,4,5-trialkyloxy-2,1-phenylene)]}tetrapalladiums and the lower substituted analogues (tetra-μ-chlorobis{μ-[1,4-phenylenebis-(nitrilomethylidenedialkyloxy-2, 1-phenylene)]}tetrapalladiums were prepared in two steps from the above bis-imine ligands and palladium(II) acetate, as described elsewhere.[6,10] Nevertheless, the yield of the second step could be improved by substituting the hydrogen chloride for lithium chloride. The intermediate complexes with acetate bridges (1.25 mmol) and fine powdered lithium chloride (47 mmol) in 200 ml of a 3 : 1 chloroform–acetone mixture were stirred for 12 h. The palladium organyls were purified by several recrystallisations from acetone–chloroform mixtures. Overall yields of the palladium organyls (starting from palladium acetate): 30–70%, depending on the chain length and the positions substituted. Melting and clearing temperatures are listed in Table 1. (Tetra-μ-chlorobis{μ-[1,4-phenylenebis(nitrilomethylidene-3, 4, 5-trialkyloxy-2,1-phenylene)]}tetrapalladiums: alkyl-hexyl: yellow powder, $C_{112}H_{172}O_{12}N_4Pd_4Cl_4$ (2334.1), C(%): 57.49 found, 57.63 calc., H(%): 7.45 found, 7.43 calc.; alkyl = octyl: yellow powder, $C_{136}H_{220}O_{12}N_4Pd_4Cl_4$ (2670.7), C(%): 60.84 found, 61.16 calc., H(%): 8.32 found, 8.30 calc.; alkyl = decyl,[10] alkyl = dodecyl,[6] alkyl = tetradecyl,[10] alkyl = hexadecyl: yellow powder, $C_{232}H_{412}O_{12}N_4Pd_4Cl_4$ (4017.3), C(%): 69.35 found, 69.36 calc., H(%): 10.32 found, 10.34 calc.; alkyl = octadecyl: yellow powder, $C_{256}H_{460}O_{12}N_4Pd_4Cl_4$ (4354.0), C(%): 70.56 found, 70.62 calc., H(%): 10.67 found, 10.65 calc.; identical ^{1}H NMR data;[6,10] also nearly identical ^{13}C NMR data.[6,10] (Tetra-μ-chlorobis{μ-[1, 4-phenylenebis(nitrilomethylidene-2, 3-dialkyloxy-2,1-phenylene)]}tetrapalladiums: alkyl = octadecyl: yellow powder, $C_{184}H_{316}O_8N_4Pd_4Cl_4$ (3280.0), C(%): 67.19 found, 67.38 calc., H(%): 9.83 found, 9.71 calc.; alkyl = dodecyl: yellow powder, $C_{136}H_{220}O_8N_4Pd_4Cl_4$ (2606.8), C(%): 62.69 found, 62.66 calc., H(%): 8.59 found, 8.51 calc.; identical ^{1}H NMR data ($CDCl_3$): $\delta = 8.21$ (s, C*H*N), 6.98, 6.76 (2d, $J = 8$ Hz, 4 aromatic H each), 7.25 (s, 8 aromatic H), 4.09, 3.93 (2t, $J = 7$ Hz, OCH_2), 1.77, 1.69 (2tt, $J = 7$ Hz, OCH_2CH_2), 1.50–1.18 (m, further CH_2 groups), 0.89, 0.87 (2t, $J = 7$ Hz, CH_3); ^{13}C NMR data ($CDCl_3$): $\delta = 172.09$ (d, 4 *C*HN groups), 148.73, 148.42, 147.28, 144.04, 139.45 (5s, 4 aromatic C each), 127.63, 117.57 (2d, 4 aromatic C each), 123.82 (d, 8 aromatic C), 74.40, 69.17 (2t, 8 OCH_2 groups), 30.90–29.35 (5t, 64 CH_2 groups), 26.16, 25.96 (2t, 8 CH_2 groups), 22.67 (t, 8 CH_2 groups), 14.09 (q, 8 CH_3 groups). (Tetra-μ-chlorobis{μ-[1,4-phenylenebis-(nitrilomethylidene-2,4-didodecyloxy-2,1-phenylene)]}tetrapalladium: yellow powder, $C_{136}H_{220}O_8N_4Pd_4Cl_4$ (2606.8), C(%): 62.66 found, 62.66 calc., H(%): 8.66 found, 8.51 calc.; ^{1}H NMR data ($CDCl_3$): $\delta = 8.08$ (s, C*H*N), 6.49, 6.02 (2s, 4 aromatic H each), 7.19 (s, 8 aromatic H), 4.03, 3.91 (2t, $J = 7$ Hz, CH_2), 1.83–1.70 (m, OCH_2CH_2), 1.50–1.18 (m, further CH_2 groups), 0.89, 0.87 (2t, $J = 7$ Hz, CH_3); ^{13}C NMR data ($CDCl_3$): $\delta = 169.96$ (d, 4 *C*HN groups), 162.04, 159.57, 158.51, 147.32, 128.08 (5s, 4 aromatic C each), 111.14, 95.61 (2d, 4 aromatic C each), 123.89 (d, 8 aromatic C), 68.32, 68.20 (2t, 8 OCH_2 groups), 31.76–29.16 (10t, 64 CH_2 groups), 26.03, 25.88 (2t, 8 CH_2 groups), 22.51, 22.49 (2t, 8 CH_2 groups), 13.81 (q, 8 CH_3 groups).

We are grateful to the Human Capital and Mobility Program (Project ERBCHRX-CT 930161 of the EU) for their financial support. K. P. also thanks the Deutsche Forschungsgemeinschaft (Sonderforschungsbereich Sfb 335 'Anisotrope Fluide', project C 6), Bonn, Germany, the Fonds der Chemischen Industrie, Frankfurt/Main, Germany, the Technische Universität Berlin, and the Gesellschaft von Freunden der Technischen Universität, as well as the Degussa AG., Hanau, Germany, for the supply of variable chemicals. We also thank Dr. P. Sebastiao for helpful discussions.

References

1 N. Usolt'seva, P. Espinet, J. Buey, K. Praefcke and D. Blunk, *Mol. Cryst. Liq. Cryst*., in the press.
2 V. Luzzati, H. Mustacchi, A. Skoulios and F. Husson, *Acta Crystallogr*., 1960, **13**, 660; P. Kékicheff and B. Cabane, *J. Phys.* (*France*), 1987, **48**, 1571; P. Kékicheff, *Mol. Cryst. Liq. Cryst*., 1991, **198**, 131.
3 B. Kohne and K. Praefcke, *Chem. Z*., 1985, **109**, 121.
4 P. Weber, D. Guillon and A. Skoulios, *Liq. Cryst*., 1991, **9**, 369.
5 M. Ibn-Elhaj, D. Guillon, A. Skoulios, A. M. Giroud-Godquin and P. Maldivi, *Liq. Cryst*., 1992, **11**, 731.
6 K. Praefcke, D. Singer and B. Gündogan, *Mol. Cryst. Liq. Cryst*., 1992, **223**, 181.
7 K. Praefcke, S. Diele, J. Pickart, B. Gündogan, U. Nütz and D. Singer, *Liq. Cryst*., 1995, **18**, 857.

8 K. Praefcke, B. Bilgin, N. Usolt'seva, B. Heinrich and D. Guillon, *J. Mater. Chem*., 1995, **5**, 2257.
9 N. Usolt'seva, K. Praefcke, D. Singer and B. Gündogan, *Liq. Cryst*., 1994, **16**, 601; N. Usolt'seva, K. Praefcke, D. Singer and B. Gündogan, *Liq. Cryst*., 1994, **16**, 617.
10 N. Usolt'seva, G. Hauck, H. D. Koswig, K. Praefcke and B. Heinrich, *Liq. Cryst*., 1996, **20**, 731.
11 *International Tables for X-Ray Crystallography*, Kluwer Academic Publishers, London, 1995.
12 K. Doolittle, *J. Appl. Phys*., 1951, **22**, 1471; H. Allouchi, M. Cotrait, D. Guillon, B. Heinrich and H. T. Nguyen, *Chem. Mater*., 1995, **7**, 2252.
13 B. Heinrich, K. Praefcke and D. Guillon, unpublished results.
14 B. Heinrich, A. Halbwachs, A. Skoulios and D. Guillon, to be published.

Paper 6/06600C; *Received* 27*th September*, 1996